93583-25-6; *i*-Pr_2NH, 108-18-9; PCl_3, 7719-12-2; $AlCl_3$, 7446-70-0; 1,3-butadiene, 106-99-0; 2,3-dimethyl-1,3-butadiene, 513-81-5; isoprene, 78-79-5; *trans*-piperylene, 2004-70-8; *trans*-2-*trans*-4-hexadiene, 5194-51-4; 1,3-cyclohexadiene, 592-57-4; 1,4-pentadiene, 591-93-5.

Supplementary Material Available: Tables of positional and isotropic thermal parameters for hydrogen atoms, anisotropic thermal parameters for non-hydrogen atoms, and observed and calculated structure factors (89 pages). Ordering information is given on any current masthead page.

Contribution from the Division of Chemical and Physical Sciences, Deakin University, Waurn Ponds, Victoria 3217, Australia, and Department of Inorganic Chemistry, University of Melbourne, Parkville, Victoria 3052, Australia

Redox Reactions of Chromium Tetracarbonyl and Tricarbonyl Complexes: Thermodynamic, Kinetic, and Catalytic Aspects of Isomerization in the *fac*/*mer*-Tricarbonyltris(trimethyl phosphite)chromium(1+/0) System

A. M. Bond,*[1] R. Colton,*[2] and J. E. Kevekordes[2]

Received July 12, 1985

Electrochemical studies have been undertaken on mixtures of *cis*- and *trans*-$[Cr(CO)_4P_2]^{+/0}$ systems (where P = P(*m*-tol)$_3$, P(*p*-tol)$_3$, P(OMe)$_3$, P(OEt)$_3$, P(OPh)$_3$). In accordance with theoretical predictions, redox potentials for both *cis*- and *trans*-$[Cr(CO)_4P_2]^{+/0}$ are similar and oxidation involves the formation of *trans*-$[Cr(CO)_4P_2]^+$ via either direct electron transfer or *cis*-$[Cr(CO)_4P_2]^+$ to *trans*-$[Cr(CO)_4P_2]^+$ isomerization after electron transfer. The *trans*-$[Cr(CO)_4P_2]^+$ species have all been identified by infrared spectroscopy. *trans*-$[Cr(CO)_4(P(OPh)_3)_2]^+$ is a very strong oxidant and can be used to oxidize all the other $[Cr(CO)_4P_2]$ complexes: *trans*-$[Cr(CO)_4(P(OPh)_3)_2]^+$ + *cis*/*trans*-$[Cr(CO)_4P_2]$ → *cis*/*trans*-$[Cr(CO)_4(P(OPh)_3)_2]$ + *trans*-$[Cr(CO)_4P_2]^+$. Tricarbonyltris(phosphorus ligand)chromium complexes, $Cr(CO)_3P_3$, can exist in *fac* or *mer* isomeric forms. In contrast to those of the tetracarbonyl complexes, the oxidation potentials of the *fac* and *mer* isomers of the tricarbonyls occur at considerably different potentials, enabling detailed electrochemical studies to be made. In this work it is shown that isomerization of *fac*-$[Cr(CO)_3(P(OMe)_3)_3]$ → *mer*-$[Cr(CO)_3(P(OMe)_3)_3]$ occurs either slowly by an intramolecular twist mechanism or via an alternative redox-catalyzed pathway. Variable-temperature electrochemical studies at platinum electrodes (cyclic voltammetry and differential-pulse voltammetry at a stationary electrode, rotating-disk voltammetry, and controlled-potential electrolysis) of the redox properties of both *fac*- and *mer*-$[Cr(CO)_3(P(OMe)_3)_3]$ provide a complete thermodynamic and kinetic description of the catalytic scheme, which involves the following reactions:

$$fac\text{-}[Cr(CO)_3(P(OMe)_3)_3] \xrightarrow{\text{oxidant}} fac\text{-}[Cr(CO)_3(P(OMe)_3)_3]^+ \quad \text{(i)}$$

where oxidant = e^-, $NOPF_6$, or *trans*-$[Cr(CO)_4(P(OPh)_3)_2]^+$

$$fac\text{-}[Cr(CO)_3(P(OMe)_3)_3]^+ \rightleftarrows mer\text{-}[Cr(CO)_3(P(OMe)_3)_3]^+ \quad \text{(ii)}$$

$$mer\text{-}[Cr(CO)_3(P(OMe)_3)_3]^+ + fac\text{-}[Cr(CO)_3(P(OMe)_3)_3] \xrightarrow{\text{fast}} fac\text{-}[Cr(CO)_3(P(OMe)_3)_3]^+ + mer\text{-}[Cr(CO)_3(P(OMe)_3)_3] \quad \text{(iii)}$$

where *fac*/*mer*-$[Cr(CO)_3(P(OMe)_3)_3]^+$ is the catalyst. Data at 22 °C in dichloromethane:

$$fac\text{-}[Cr(CO)_3(P(OMe)_3)_3] \underset{k_{-1}}{\overset{k_1}{\rightleftharpoons}} mer\text{-}[Cr(CO)_3(P(OMe)_3)_3]$$

$$k_1 = (1.8 \pm 0.3) \times 10^{-4}\ s^{-1} \qquad k_{-1} = (4.5 \pm 1.3) \times 10^{-5}\ s^{-1} \qquad K_1 = 4 \pm 0.5$$

$$fac\text{-}[Cr(CO)_3(P(OMe)_3)_3]^+ \underset{k_{-2}}{\overset{k_2}{\rightleftharpoons}} mer\text{-}[Cr(CO)_3(P(OMe)_3)_3]^+$$

$$k_2 = 0.11 \pm 0.01 \qquad k_{-2} = (1.7 \pm 0.8) \times 10^{-4}\ s^{-1} \qquad K_2 = 640 \pm 130$$

The activation parameters for *fac*-$[Cr(CO)_3(P(OMe)_3)_3]^+ \rightleftarrows$ *mer*-$[Cr(CO)_3(P(OMe)_3)_3]^+$ are consistent with those expected for an intramolecular twist mechanism (E_A = 15.9 ± 0.7 kJ/mol; ΔS^* = −17.0 ± 1.0 J/(K mol)). The equilibrium constant, K_3, for the redox cross-reaction

$$fac\text{-}[Cr(CO)_3(P(OMe)_3)_3]^+ + mer\text{-}[Cr(CO)_3(P(OMe)_3)_3] \underset{}{\overset{K_3}{\rightleftharpoons}} fac\text{-}[Cr(CO)_3(P(OMe)_3)_3] + mer\text{-}[Cr(CO)_3(P(OMe)_3)_3]^+$$

has a value of 160 ± 13. The electrochemical properties of *fac*/*mer*-$[Cr(CO)_3(P(OEt)_3)_3]$ are similar.

Introduction

There is a considerable interest in the interplay between steric and electronic effects determining the isomeric form of octahedral carbonyl complexes.[3,4] In addition, extensive studies have been made of the substituent effects of the groups attached to the donor atom on the thermodynamic aspects of the electrochemical oxidation or reduction of these complexes.[3,5,6]

In the particular case of the group VI (group 6[22]) tetracarbonyl and tricarbonyl species, $M(CO)_4P_2$ and $M(CO)_3P_3$ (M = Cr, Mo,

(1) Deakin University.
(2) University of Melbourne.
(3) Bursten, B. E. *J. Am. Chem. Soc.* **1982**, *104*, 1299 and references cited therein.
(4) Mingos, D. M. P. *J. Organomet. Chem.* **1979**, *179*, C29.
(5) (a) Butler, G.; Chatt, J.; Leigh, G. J.; Pickett, C. J. *J. Chem. Soc., Dalton Trans.* **1979**, 113. (b) Chatt, J.; Leigh, G. J.; Neukomm, H.; Pickett, C. J.; Stanley, D. R. *J. Chem. Soc., Dalton Trans.* **1980**, 121. (c) Crichton, B. A. L.; Dilworth, J. R.; Pickett, C. J.; Chatt, J. *J. Chem. Soc., Dalton Trans.* **1981**, 419. (d) Leigh, G. J.; Morris, R. H.; Pickett, C. J.; Stanley, D. R.; Chatt, J. *J. Chem. Soc., Dalton Trans.* **1981**, 800.
(6) Pombeiro, A. J. L. *Port. Electrochim. Acta* **1983**, *1*, 19.

0020-1669/86/1325-0749$01.50/0

W; P = monodentate phosphorus ligand), the cis/fac arrangement is preferred on electronic grounds, but the trans/mer isomer may be the thermodynamically stable form due to steric effects from the bulky ligands.[7-9] There is a substantial quantity of literature available on the isomerization rates and the mechanism of isomerization of these 18-electron species and closely related substitution reactions (see for example ref 9–12), and it is generally concluded that the isomerizations occur via an intramolecular twist mechanism. In contrast, there is no quantitative information available on the corresponding oxidized 17-electron $[M(CO)_4P_2]^+$ or $[M(CO)_3P_3]^+$ species as is required for a complete thermodynamic and kinetic description of the total redox system nor is any information available on reactions of oxidized tetracarbonyl complexes with 18-electron tricarbonyl species.

It has been predicted that $E°$ values for the redox couples associated with cis and trans tetracarbonyl isomers

$$cis\text{-}[M(CO)_4P_2]^+ + e^- \overset{E_1°}{\rightleftharpoons} cis\text{-}[M(CO)_4P_2] \quad (1)$$

$$trans\text{-}[M(CO)_4P_2]^+ + e^- \overset{E_2°}{\rightleftharpoons} trans\text{-}[M(CO)_4P_2] \quad (2)$$

should be identical.[3] Furthermore, the $E°$ values are predicted to be considerably more positive than for tricarbonyl species so that, thermodynamically at least, reactions of the kind

$$[M(CO)_4P_2]^+ + M(CO)_3P_3 \rightarrow M(CO)_4P_2 + [M(CO)_3P_3]^+ \quad (3)$$

could be expected to occur, although whether they will occur, because of kinetic considerations, is uncertain. In contrast to the similarities of $E_1°$ and $E_2°$, $E_3°$ and $E_4°$ for the reactions

$$fac\text{-}[M(CO)_3P_3]^+ + e^- \overset{E_3°}{\rightleftharpoons} fac\text{-}[M(CO)_3P_3] \quad (4)$$

$$mer\text{-}[M(CO)_3P_3]^+ + e^- \overset{E_4°}{\rightleftharpoons} mer\text{-}[M(CO)_3P_3] \quad (5)$$

are predicted to be measurably different, with $E_3°$ being the more positive.[3] Thus the thermodynamics of the reaction indicated by eq 3 may vary, depending on the isomeric distributions of reactant and product.

Clearly, a delicate balance exists between thermodynamic and kinetic parameters in each of the oxidation states 0 and I[13] for both tetracarbonyl and tricarbonyl group VI metal complexes. Since $E_1°$ and $E_2°$ are expected to be very similar, and $E_3°$ and $E_4°$ measurably different, catalyatic isomerization schemes involving electron transfer may occur. Generation of $[M(CO)_3P_3]^+$ via electrolysis, or via a chemical redox process of the type described by eq 3, may provide an alternative and faster route for isomerization of the thermodynamically unfavored 18-electron tricarbonyl isomer, rather than the simple intramolecular rearrangement that occurs slowly in solution.

We have previously reported detailed electrochemical studies on the *trans*-$[Cr(CO)_4(PPh_3)_2]^{+/0}$[14] and *fac*/*mer*-$[Cr(CO)_3P_3]^{+/0}$[15] redox systems. In the present work, a series of *trans*-$[Cr(CO)_4P_2]$ (or mixtures of *cis*- and *trans*-$[Cr(CO)_4P_2]$) species and their new corresponding cations *trans*-$[Cr(CO)_4P_2]^+$ [P = PPh_3, P(*m*-tol)$_3$, P(*p*-tol)$_3$, $P(OPh)_3$, $P(OEt)_3$, $P(OMe)_3$] have been characterized by infrared and NMR spectroscopy and investigated by electrochemical techniques to establish the thermodynamic and kinetic characteristics of both the 18- and 17-electron species. Redox reactions relating them, and possible redox-based catalytic schemes[15] for isomerization of *fac*-$[Cr(CO)_3(P(OMe)_3)_3]$, induced either electrochemically or by reaction with $NOPF_6$ or *trans*-$[Cr(CO)_4P_2]^+$, also have been investigated quantitatively.

Experimental Section

Materials. All solvents were of AR grade and were dried over 4A molecular sieves. $Cr(CO)_6$ and the phosphorus ligands were obtained commercially and were used without further purification. *trans*-$[Cr(CO)_4P_2]$ complexes were prepared by literature methods;[9,16,17] on dissolution equilibrium mixtures of cis and trans isomers were obtained in some cases as described in the text. *trans*-$[Cr(CO)_4(PPh_3)_2]^+$ was prepared as described previously.[14] Other *trans*-$[Cr(CO)_4P_2]^+$ complexes were generated in the electrochemical cell by the following two methods: (a) A slight excess of $AgClO_4$ was added to a dichloromethane solution of *trans*-$[Cr(CO)_4P_2]$ under a nitrogen atmosphere in the absence of light. Dark blue (P = P(*p*-tolyl)$_3$, P(*m*-tolyl)$_3$), violet (P = $P(OPh)_3$), or yellow ($P(OMe)_3$, $P(OEt)_3$) solutions of *trans*-$[Cr(CO)_4P_2]^+$ were produced. $NOPF_6$ gives similar results except for the cases $Cr(CO)_4P_2$ (P = $P(OMe)_3$, $P(OEt)_3$); in these systems nitrosyl substitution products are obtained. (b) Oxidative-controlled-potential electrolysis of dichloromethane solutions of *trans*-$[Cr(CO)_4P_2]$ gave similarly colored solutions to those described in method a. These 17-electron cations were not isolated from the solutions due to their limited stability. *fac*/*mer*-$[Cr(CO)_3P_3]$ complexes were prepared by literature methods.[15] Oxidation to the 17-electron cations was carried out as described for the tetracarbonyls or was carried out by oxidation using *trans*-$[Cr(CO)_4(P(OPh)_3)_2]^+$ (see later text).

Instrumentation. Electrochemical Measurements. Voltammograms were obtained in dichloromethane (0.1 M Bu_4NClO_4) by using a Princeton E.G. and G. (PAR) Model 174A polarographic analyzer and a conventional three-electrode cell at 22 °C unless otherwise stated. For cyclic voltammetry, the platinum working electrode was in the form of a disk or wire and used in a stationary mode. The reference electrode was Ag/AgCl (EtOH; saturated LiCl) separated from the test solution by a salt bridge (0.1 M Bu_4NClO_4 in CH_2Cl_2). Frequent calibration of this reference electrode was carried out against a standard ferrocene solution. The auxiliary electrode was a platinum wire. All solutions were degassed with nitrogen and maintained under a nitrogen atmosphere throughout the measurements. For variable-temperature cyclic voltammetry the temperature was regulated with an acetone/dry ice bath, the temperature being monitored with a calibrated thermocouple. For steady-state experiments, a Metrohm platinum rotating disk electrode with variable rotation rates was used with the same auxiliary and working electrodes as above. Controlled-potential electrolysis experiments were performed with a PAR Model 173 potentiostat/galvanostat. A PAR Model 179 digital coulometer was used in conjunction with this potentiostat. A three-electrode configuration was used with a platinum-gauze working electrode in all controlled-potential electrolysis experiments. Potentials were set against the Ag/AgCl reference electrode. The auxiliary electrode was constructed from platinum gauze separated from the bulk solution by a salt bridge containing a porous Vycor plug. The solutions were continuously purged with nitrogen and kept in darkness during the electrolysis.

Spectroscopic Measurements. Infrared spectra were recorded on a Jasco A 302 spectrometer and calibrated against polystyrene. NMR spectra were recorded on a JEOL FX 100 spectrometer using an external ^7Li lock. Carbon-13 NMR spectra were recorded in $CDCl_3$ solution at 25.048 MHz and referenced against Me_4Si. $Cr(acac)_3$ was added as a paramagnetic relaxant. Phosphorus-31 NMR spectra were recorded at 40.32 MHz with 85% H_3PO_4 as reference. Chemical shifts are reported by using the high frequency positive convention.

Results and Discussion

All studies were carried out in dichloromethane solution unless otherwise stated.

Preparation and Characterization. Infrared spectra in the carbonyl region clearly distinguish between *cis*/*trans*-$[Cr(CO)_4P_2]$

(7) Darensbourg, D. J.; Kump, R. L. *Inorg. Chem.* **1978**, *17*, 2680.
(8) Dixon, D. T.; Burkinshaw, P. M.; Howell, J. A. S. *J. Chem. Soc., Dalton Trans.* **1980**, 2237.
(9) Dixon, D. T.; Kola, J. C.; Howell, J. A. S. *J. Chem. Soc., Dalton Trans.* **1984**, 1307.
(10) (a) Darensbourg, D. J. *Inorg. Chem.* **1979**, *18*, 14. (b) Cotton, F. A.; Darensbourg, D. J.; Klein, S.; Kolthammer, B. W. S. *Inorg. Chem.* **1982**, *21*, 2661. (c) Darensbourg, D. J.; Gray, R. L.; *Inorg. Chem.* **1984**, *23*, 2993.
(11) (a) Darensbourg, D. J.; Graves, A. H. *Inorg. Chem.* **1979**, *18*, 1257. (b) Darensbourg, D. J.; Kudaroski, R.; Schenk, W. *Inorg. Chem.* **1982**, *21*, 2488.
(12) (a) Wovkulich, M. J.; Feinberg, S. J.; Atwood, J. D. *Inorg. Chem.* **1980**, *19*, 2608. (b) Atwood, J. D.; Wovkulich, M. J.; Sonnenberger, D. C. *Acc. Chem. Res.* **1983**, *16*, 350.
(13) Bond, A. M.; Darensbourg, D. J.; Mocellin, E.; Stewart, B. J. *J. Am. Chem. Soc.* **1981**, *103*, 6827.
(14) Bagchi, R. N.; Bond, A. M.; Brain, G.; Colton, R.; Henderson, T. L. E.; Kevekordes, J. E. *Organometallics* **1984**, *3*, 4.
(15) Bond, A. M.; Carr, S. W.; Colton, R. *Inorg. Chem.* **1984**, *23*, 2343.
(16) Behrens, H.; Klek, W. Z. *Z. Anorg. Allg. Chem.* **1957**, *292*, 151.
(17) Mathieu, R.; Lenzi, M.; Poilblanc, R. *Inorg. Chem.* **1970**, *9*, 2032.

Table I. Infrared Carbonyl Stretching Frequencies and ^{31}P and ^{13}C (Carbonyl) NMR Data for Tetracarbonyl- and Tricarbonylchromium Complexes at 25 °C

compd	IR data[a,b] ν_{CO}, cm^{-1}	NMR data[c] $\delta(^{31}P)$[d]	$\delta(^{13}C)$[e]
trans-$[Cr(CO)_4(PPh_3)_2]$	1890	73.1	223.2
trans-$[Cr(CO)_4(P(m\text{-tol})_3)_2]$	1885	72.9	220.9
trans-$[Cr(CO)_4(P(p\text{-tol})_3)_2]$	1885	71.5	223.6
trans-$[Cr(CO)_4(P(OPh)_3)_2]$	1930	179.6	216.6
trans-$[Cr(CO)_4(P(OEt)_3)_2]$	1902	189.4	
trans-$[Cr(CO)_4(P(OMe)_3)_2]$	1908	193.4	219.3[h]
mer-$[Cr(CO)_3(P(OMe)_3)_3]$[f,g]	1981 (m)	196.8	226.9
	1900 (sh), 1878 (s)	188.3	221.3
cis-$[Cr(CO)_4(P(OEt)_3)_2]$	2040 (s), 1930 (sh)	175.1	
	1905 (s), 1880 (sh)		
cis-$[Cr(CO)_4(P(OMe)_3)_2]$	2030 (s), 1940 (sh)	183.1	223.6[i,j]
	1910 (s), 1870 (sh)		
cis-$[Cr(CO)_4(P(OPh)_3)_2]$	2040 (s), 1955 (sh)	172.3	
	1930 (s), 1905 (sh)		
fac-$[Cr(CO)_3(P(OMe)_3)_3]$[f]	1961 (s), 1869 (s)	185.0	226.2
trans-$[Cr(CO)_4(PPh_3)_2]^+$[k]	1980		
trans-$[Cr(CO)_4(P(p\text{-tol})_3)_2]^+$	1975		
trans-$[Cr(CO)_4(P(OPh)_3)_2]^+$	2080		
trans-$[Cr(CO)_4(P(OEt)_3)_2]^+$	2080		
trans-$[Cr(CO)_4(P(OMe)_3)_2]^+$	2080		
mer-$[Cr(CO)_3(P(OMe)_3)_3]^+$[f]	2051 (m), 1988 (m)		
	1935 (s)		

[a] In CH_2Cl_2 solution and calibrated against polystyrene, 1601-cm^{-1} band. [b] Key: s = strong, m = medium; sh = shoulder. [c] Error = 0.1 ppm. [d] In CH_2Cl_2 solution. [e] In $CDCl_3$ solution. [f] Quoted from ref 15. [g] $^2J_{P-P}$ = 60.3 Hz. [h] $^2J_{P-P}$ = 20.5 Hz. [i] $^2J_{P-P}$ = 12.7 Hz. [j] Second signal overlapped by trans signal. [k] Quoted from ref 14.

and *fac*/*mer*-$[Cr(CO)_3P_3]$ geometries. Phosphorus-31 NMR also clearly distinguishes between the isomers and may be used to follow the isomerization of 18-electron species.[9] These data are given in Table I.

All the 17-electron species $[Cr(CO)_4P_2]^+$ and $[Cr(CO)_3P_3]^+$ may be prepared by electrochemical oxidation and, in most cases, $NOPF_6$ or $AgClO_4$ oxidation of the 18-electron species. The 17-electron species obtained in all cases are the *trans*-tetracarbonyl and *mer*-tricarbonyl cations respectively (infrared data given in Table I) irrespective of the geometry of the starting material.

Electrochemical Measurements. Electrochemical data are summarized in Table II.

(a) *cis*/*trans*-$[Cr(CO)_4(P(OMe)_3)_2]$. NMR and IR data on $Cr(CO)_4(P(OMe)_3)_2$ show that there is an equilibrium mixture of cis and trans isomers in solution. Equilibrium and rate constant data for the reaction

$$cis\text{-}[Cr(CO)_4(P(OMe)_3)_2] \underset{k_{-1}}{\overset{k_1}{\rightleftharpoons}} trans\text{-}[Cr(CO)_4(P(OMe)_3)_2]$$
$$K = k_1/k_{-1} \quad (6)$$

have been reported[9] at 28 °C in toluene to be $K = 4.78$, $k_1 = 10.5 \times 10^{-4}$ s^{-1} and $k_{-1} = 2.19 \times 10^{-4}$ s^{-1}. Data in this work in dichloromethane are qualitatively consistent with these values although $K = 1.86 \pm 0.01$ in dichloromethane at 25 °C, suggesting that the cis isomer is more favored in this solvent.

Cyclic and oxidative differential-pulse voltammograms for $[Cr(CO)_4(P(OMe)_3)_2]$ in dichloromethane over the temperature range −70 to 25 °C are consistent with a one-electron oxidation (Figure 1) despite the fact that the oxidation of a mixture of isomers is occurring. For the similar $Mo(CO)_4P_2$ systems[13] subtle distinctions between the two isomers could be observed at low temperatures for some of the complexes. However, at a platinum rotating disk electrode a sigmoidal-shaped curve exhibiting Nernstian response is observed for the mixture of chromium tetracarbonyls at all temperatures, which has the same limiting current per unit concentration as the known[14] one-electron oxidation

$$trans\text{-}[Cr(CO)_4(PPh_3)_2] \rightleftharpoons trans\text{-}[Cr(CO)_4(PPh_3)_2]^+ + e^- \quad (7)$$

Coulometric measurements coupled with oxidative controlled-potential electrolysis at 1.2 V vs. Ag/AgCl in dichloromethane confirms that the oxidation of *cis*/*trans*-$[Cr(CO)_4(P(OMe)_3)_2]$ is a one-electron process, and the product formed is pure *trans*-$[Cr(CO)_4(P(OMe)_3)_2]^+$ (infrared evidence, Table I). Figure 1a shows the cyclic voltammogram for the oxidation of a mixture of *cis*- and *trans*-$[Cr(CO)_4(P(OMe)_3)_2]$. Figure 1b shows that the reductive cyclic voltammogram of the trans$^+$ species has the identical shape and position as has the oxidation of the cis/trans 18-electron mixture, the only difference being the sign of the current. Parts c and d + d of Figure 1 show that the differential-pulse voltammograms before and after oxidation are identical except for the sign of the current. Infrared spectra confirm that after controlled potential reduction of the pure trans$^+$ species at 0.70 V vs. Ag/AgCl, the equilibrium mixture of *cis*/*trans*-$[Cr(CO)_4(P(OMe)_3)_2]$ is reestablished. The above data may be explained by assuming that the $E°$ values for the processes

$$cis\text{-}[Cr(CO)_4(P(OMe)_3)_2]^+ + e^- \rightleftharpoons cis\text{-}[Cr(CO)_4(P(OMe)_3)_2] \quad (8)$$

$$trans\text{-}[Cr(CO)_4(P(OMe)_3)_2]^+ + e^- \rightleftharpoons trans\text{-}[Cr(CO)_4(P(OMe)_3)_2] \quad (9)$$

are similar as predicted[3] and that electrochemical oxidation of the mixture occurs in the following manner:[21]

$$\begin{array}{ccc} trans\text{-}[Cr(CO)_4(P(OMe)_3)_2] & \rightleftharpoons & trans\text{-}[Cr(CO)_4(P(OMe)_3)_2]^+ + e^- \\ \text{slow}\ \Big\downarrow\Big\uparrow\ \text{slow} & & \uparrow\ \text{fast} \\ cis\text{-}[Cr(CO)_4(P(OMe)_3)_2] & \rightleftharpoons & cis\text{-}[Cr(CO)_4(P(OMe)_3)_2]^+ + e^- \end{array} \quad (10)$$

Table II. Electrochemical Data for the Oxidation of Tetracarbonyl- and Tricarbonylchromium Complexes at a Platinum Electrode in CH_2Cl_2 (0.1 M Bu_4NClO_4) at 22 °C

compd	cyclic voltammetry[a-c] E_p^{ox}, V vs. Ag/AgCl	E_p^{red}, V vs. Ag/AgCl	$E^r_{1/2}$, V vs. Ag/AgCl	rotating disk electrode[d] $E_{1/2}$, V vs. Ag/AgCl	$E_{3/4} - E_{1/4}$, V vs. Ag/AgCl
cis/*trans*-$[Cr(CO)_4(P(OMe)_3)_2]$	0.92	0.83	0.87	0.94	0.12
cis/*trans*-$[Cr(CO)_4(P(OEt)_3)_2]$	0.88	0.67	0.78		
trans-$[Cr(CO)_4(PPh_3)_2]$	0.80	0.49	0.65	0.74	0.10
trans-$[Cr(CO)_4(P(m\text{-tol})_3)_2]$	0.66	0.52	0.59	0.60	0.08
trans-$[Cr(CO)_4(P(p\text{-tol})_3)_2]$	0.65	0.55	0.60	0.61	0.08
trans-$[Cr(CO)_4(P(OPh)_3)_2]$	1.26	1.02	1.14	1.21	0.16
mer-$[Cr(CO)_3(P(OEt)_3)_3]$	0.31	0.20	0.26		
mer-$[Cr(CO)_3(P(OMe)_3)_3]$	0.42	0.35	0.39	0.43	0.08
fac-$[Cr(CO)_3(P(OEt)_3)_3]$	0.47				
fac-$[Cr(CO)_3(P(OMe)_3)_3]$	0.57[f]	0.47[e]	0.52	0.55	0.08

[a] Scan rate = 200 mV/s. [b] $E_{1/2}$ for oxidation of $\simeq 10^{-3}$ M ferrocene vs. Ag/AgCl = 0.52 V. [c] E_p^{ox} = oxidation potential of forward scan of cyclic voltammogram; E_p^{red} = reduction potential of reverse scan of cyclic voltammogram; $E^r_{1/2}$ = calculated reversible half-wave potential; $E_{3/4}$ and $E_{1/4}$ = potential at $^3/_4$ and $^1/_4$ of the limiting current value, respectively. [d] Rotation rate of platinum electrode = 2000 cycles/min. [e] Calculated from data obtained at −60 °C. [f] Reference 15.

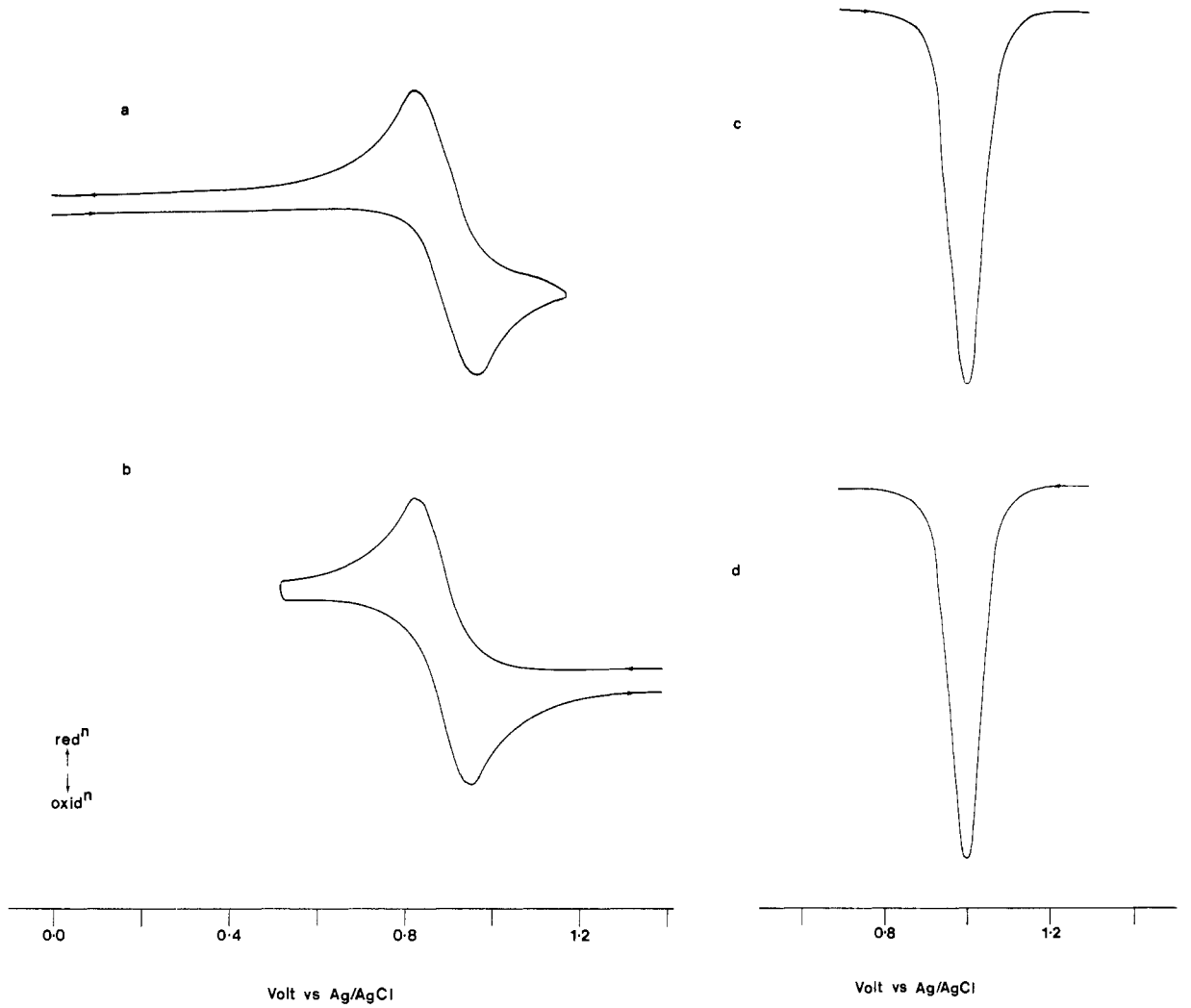

Figure 1. (a) Cyclic voltammogram (scan rate = 200 mV/s) for oxidation of a mixture of *cis*/*trans*-$[Cr(CO)_4(P(OMe)_3)_2]$. (b) Cyclic voltammogram (scan rate = 200 mV/s) for reduction of *trans*-$[Cr(CO)_4(P(OMe)_3)_2]^+$. (c) Oxidative differential-pulse voltammogram (scan rate = 5 mV/s; duration between pulses = 0.5 s; pulse amplitude = 10 mV) of a mixture of *cis*/*trans*-$[Cr(CO)_4(P(OMe)_3)_2]$. (d) Reductive differential-pulse voltammogram with display direction inverted (same conditions as part c, except for pulse sign) of *trans*-$[Cr(CO)_4(P(OMe)_3)_2]^+$. All solutions had compound concentrations $\sim 2 \times 10^{-4}$ M in dichloromethane at 22 °C. A stationary platinum electrode was used.

The reduction of *trans*-$[Cr(CO)_4(P(OMe)_3)_2]^+$ is then described by

$$trans\text{-}[Cr(CO)_4(P(OMe)_3)_2]^+ + e^- \rightleftarrows trans\text{-}[Cr(CO)_4(P(OMe)_3)_2] \underset{\text{slow}}{\overset{\text{slow}}{\rightleftharpoons}} cis\text{-}[Cr(CO)_4(P(OMe)_3)_2] \quad (11)$$

On oxidation of mixtures of *cis*- and *trans*-$[Cr(CO)_4(P(OMe)_3)_2]$ with $NOPF_6$, quantitative conversion to the *trans*-$[Cr(CO)_4(P(OMe)_3)_2]^+$ occurs as required by the above reaction scheme.

(b) *trans*-$[Cr(CO)_4P_2]$ (P = P(*m*-tol)$_3$, P(*p*-tol)$_3$). These complexes can only be isolated in the trans configuration due to the bulky nature of the phosphine ligands. Electrochemical data are summarized in Table II, and all are similar to those for the previously reported[14] reversible one-electron oxidation described in eq 7. No evidence for the corresponding cis isomers was detected, even after electrochemical oxidation and reduction sequences, consistent with observations from the original synthesis, which implies the equilibrium constant strongly favors the trans isomer.

(c) *trans*-$[Cr(CO)_4(P(OPh)_3)_2]$. Again, due to the bulky nature of the phosphite ligand, the trans isomer is strongly favored and the cis isomer was not isolated in agreement with previous reports, although the presence of small amounts of the cis isomer can be observed in the infrared spectra of solutions[9] (Table I). The cyclic voltammograms, oxidation curves at a platinum rotating disk electrode, and chemical oxidation by $NOPF_6$ of freshly prepared solutions of *trans*-$[Cr(CO)_4(P(OPh)_3)_2]$ are very similar to those of the *trans*-$[Cr(CO)_4(P(OMe)_3)_2]$ system described earlier. However, the E° value of 1.14 V vs. Ag/AgCl for the one-electron reversible oxidation of *trans*-$[Cr(CO)_4(P(OPh)_3)_2]$ is considerably more positive than for the other complexes considered in this report (Table II) and is too positive for $AgClO_4$ to be used as an oxidant. The solution of *trans*-$[Cr(CO)_4(P(OPh)_3)_2]^+$ is violet in color, and its infrared spectrum shows a single carbonyl stretch at 2080 cm^{-1}, a shift of 150 cm^{-1} relative to the peak for *trans*-$[Cr(CO)_4(P(OPh)_3)_2]$. Oxidative controlled-potential electrolysis of *trans*-$[Cr(CO)_4(P(OPh)_3)_2]$, even in the dark and under nitrogen, yielded apparent values of $n > 1$, due to the light and chemical sensitivity of the 17-electron species. Similar behavior has been previously observed for *trans*-$[Cr(CO)_4(PPh_3)_2]$.[14]

(18) Bond, A. M.; Colton, R.; Jackowski, J. J. *Inorg. Chem.* **1975**, *14*, 2526.
(19) Nicholson, R. S.; Shain, I. *Anal. Chem.* **1964**, *36*, 706.
(20) Bond, A. M.; Grabaric, B. S.; Jackowski, J. J. *Inorg. Chem.* **1978**, *17*, 2153.
(21) It should be noted that when thermodynamic relationships are discussed, the IUPAC convention of writing redox reactions as reduction processes has been followed. However, when voltammetric experiments are described, the reactions are written either as oxidation or reduction steps to reflect the true nature of the experiments actually undertaken.
(22) In this paper the periodic group notation in parentheses is in accord with recent actions by IUPAC and ACS nomenclature committees. A and B notation is eliminated because of wide confusion. Groups IA and IIA become groups 1 and 2. The d-transition elements comprise groups 3 through 12, and the p-block elements comprise groups 13 through 18. (Note that the former Roman number designation is preserved in the last digit of the new numbering: e.g., III → 3 and 13.)

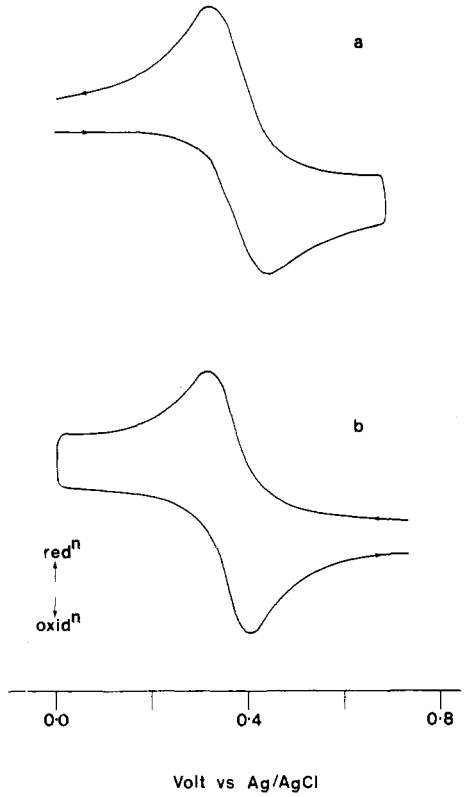

Figure 2. Cyclic voltammograms (scan rate = 200 mV/s) in dichloromethane at 22 °C using a stationary platinum electrode: (a) oxidation of $\simeq 2 \times 10^{-4}$ M *mer*-$[Cr(CO)_3(P(OMe)_3)_3]$; (b) reduction of $\simeq 2 \times 10^{-4}$ M *mer*-$[Cr(CO)_3(P(OMe)_3)_3]^+$.

The large positive $E°$ value for the *trans*-$[Cr(CO)_4(P(OPh)_3)_2]^{+/0}$ couple led to *trans*-$[Cr(CO)_4(P(OPh)_3)_2]^+$ being used as an oxidant for the other complexes studied in this work. Electrochemical monitoring of the reaction of *trans*-$[Cr(CO)_4(P(OPh)_3)_2]^+$ with *trans*-$[Cr(CO)_4(PPh_3)_2]$ cannot give any useful information since both trans$^{+/0}$ couples are completely reversible. However, the reaction could be monitored qualitatively by infrared spectroscopy. Upon mixing, the two well-defined absorbances due to *trans*-$[Cr(CO)_4(P(OPh)_3)_2]^+$ (2080 cm^{-1}) and *trans*-$[Cr(CO)_4(PPh_3)_2]$ (1890 cm^{-1}) decreased in intensity while absorbances at the known positions for *trans*-$[Cr(CO)_4(P(OPh)_3)_2]$ (1930 cm^{-1}) and *trans*-$[Cr(CO)_4(PPh_3)_2]^+$ (1980 cm^{-1})[14] appeared and increased in intensity with time. The solution immediately changed from violet to the intense dark blue of *trans*-$[Cr(CO)_4(PPh_3)_2]^+$.[14] These results indicated that the following reaction occurs:

$$\textit{trans}\text{-}[Cr(CO)_4(PPh_3)_2] + \textit{trans}\text{-}[Cr(CO)_4(P(OPh)_3)_2]^+ \rightarrow \textit{trans}\text{-}[Cr(CO)_4(PPh_3)_2]^+ + \textit{trans}\text{-}[Cr(CO)_4(P(OPh)_3)_2] \quad (12)$$

After 10 min no trace of *trans*-$[Cr(CO)_4(PPh_3)_2]$ or *trans*-$[Cr(CO)_4(P(OPh)_3)_2]^+$ remained in solution, and it appeared that a complete reaction had occurred as would be expected from the $E°$ values for the respective couples.

(d) *mer*-$[Cr(CO)_3(P(OMe)_3)_3]^{+/0}$. A description of some aspects of the electrochemistry of this compound is available in ref 15, although the time dependence of the data has yet to be considered. Also, no quantitative data were reported on equilibrium or rate constants for the various processes in the previous study. These latter aspects, as well as the consequences of undertaking oxidation and reduction cycles, provide considerably more detailed understanding of the redox chemistry than is available from data in the literature. Figure 2a shows a cyclic voltammogram for the first oxidation process of a freshly prepared CH_2Cl_2 solution of *mer*-$[Cr(CO)_3(P(OMe)_3)_3]$ at 22 °C. The chemically reversible couple has peak to peak characteristics that are very similar to those for the one-electron oxidation of ferrocene; the process is therefore defined as electrochemically reversible. Importantly,

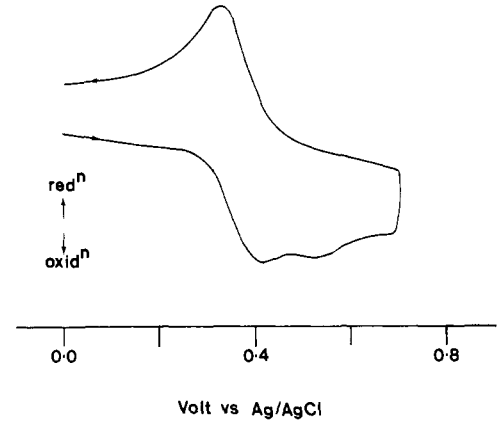

Figure 3. Cyclic voltammogram (scan rate = 200 mV/s) after oxidative controlled-potential electrolysis of $\simeq 2 \times 10^{-4}$ M *mer*-$[Cr(CO)_3(P(OMe)_3)_3]$ at 0.6 V vs. Ag/AgCl followed by reductive controlled-potential electrolysis at 0.0 V vs. Ag/AgCl in dichloromethane at 22 °C using a stationary platinum electrode.

the $E°$ value (Table II) is observed to be considerably less positive than for the analogous tetracarbonyl complex considered in section a and as expected from theoretical considerations.[3]

Controlled-potential electrolysis at 0.6 V vs. Ag/AgCl of the freshly prepared and initially colorless solution produced a yellow solution, which then gave a reversible reduction cyclic voltammogram with the same $E_{1/2}$ value as found for the initial oxidation (Figure 2b), thus confirming the chemical reversibility of the couple

$$\textit{mer}\text{-}[Cr(CO)_3(P(OMe)_3)_3] \rightleftarrows \textit{mer}\text{-}[Cr(CO)_3P((OMe)_3)_3]^+ + e^- \quad (13)$$

for short timescale experiments. The infrared spectrum (Table I) of *mer*-$[Cr(CO)_3(P(OMe)_3)_3]^+$ obtained by the oxidation of *mer*-$[Cr(CO)_3(P(OMe)_3)_3]$ in dichloromethane solution shows three carbonyl stretches all moved to higher frequencies relative to the zerovalent *mer*-$[Cr(CO)_3(P(OMe)_3)_3]$ complex consistent with the literature data.[15]

The chemical oxidation of freshly prepared *mer*-$[Cr(CO)_3(P(OMe)_3)_3]$ with *trans*-$[Cr(CO)_4(P(OPh)_3)_2]^+$ at 22 °C was monitored with a platinum rotating disk electrode and by infrared spectroscopy. The one-electron-oxidation process initially observed is gradually transformed into the corresponding reduction wave with no change in $E_{1/2}$, thus unequivocally confirming the chemical and electrochemical reversibility of the *mer*-$[Cr(CO)_3(P(OMe)_3)_3]^{+/0}$ redox couple. Furthermore, a combination of electrochemical and infrared monitoring demonstrates that the reaction

$$\textit{mer}\text{-}[Cr(CO)_3(P(OMe)_3)_3] + \textit{trans}\text{-}[Cr(CO)_4(P(OPh)_3)_2]^+ \rightarrow \textit{mer}\text{-}[Cr(CO)_3(P(OMe)_3)_3]^+ + \textit{trans}\text{-}[Cr(CO)_4(P(OPh)_3)_2] \quad (14)$$

occurs. With $NOPF_6$, the reaction

$$\textit{mer}\text{-}[Cr(CO)_3(P(OMe)_3)_3] + NOPF_6 \rightarrow \textit{mer}\text{-}[Cr(CO)_3(P(OMe)_3)_3]PF_6 + NO \quad (15)$$

has been shown to be quantitative as would be expected with this strong oxidant.

Controlled-potential reductive electrolysis of *mer*-$[Cr(CO)_3(P(OMe)_3)_3]^+$ at 0.0 V vs. Ag/AgCl over a time period of 10 min produces a mixture of *fac*- and *mer*-$[Cr(CO)_3(P(OMe)_3)_3]$. An oxidative cyclic voltammogram of this solution is shown in Figure 3, and it is distinguished from Figure 2a by an additional oxidation process approximately 100 mV more positive than for the oxidation of *mer*-$[Cr(CO)_3(P(OMe)_3)_3]$, which is the oxidation of the *fac* isomer.[15] Repeated controlled-potential oxidation at 0.6 V followed by reduction at 0.0 V vs. Ag/AgCl over six cycles always gave a pure *mer*$^{+/0}$ couple for the oxidized solution and a curve identical with Figure 3 for the reduced solution. The controlled-potential

oxidation/reduction cycles referred to above, suggest that the components of the reduced solution are in equilibrium, with the *mer* isomer dominant. Consistent with this hypothesis it was observed that the electrochemistry of initially pure *mer*-$[Cr(CO)_3(P(OMe)_3)_3]$, on standing in CH_2Cl_2 solution, exhibits a time-dependent response until ultimately a response identical with that observed in Figure 3 is obtained. NMR experiments are also consistent with the electrochemical data.

Reaction of this equilibrium mixture with *trans*-$[Cr(CO)_4(P(OPh)_3)_2]^+$ demonstrates that a chemical redox reaction occurs that can be fully explained by the following reactions:

$$mer\text{-}[Cr(CO)_3(P(OMe)_3)_3] \rightleftarrows fac\text{-}[Cr(CO)_3(P(OMe)_3)_3] \quad (16)$$

$$mer\text{-}[Cr(CO)_3(P(OMe)_3)_3] + trans\text{-}[Cr(CO)_4(P(OPh)_3)_2]^+ \rightarrow mer\text{-}[Cr(CO)_3(P(OMe)_3)_3]^+ + trans\text{-}[Cr(CO)_4(P(OPh)_3)_2] \quad (17)$$

$$fac\text{-}[Cr(CO)_3(P(OMe)_3)_3] + trans\text{-}[Cr(CO)_4(P(OPh)_3)_2]^+ \rightarrow fac\text{-}[Cr(CO)_3(P(OMe)_3)_3]^+ + trans\text{-}[Cr(CO)_4(P(OPh)_3)_2] \quad (18)$$

$$fac\text{-}[Cr(CO)_3(P(OMe)_3)_3]^+ \rightarrow mer\text{-}[Cr(CO)_3(P(OMe)_3)_3]^+ \quad (19)$$

$$trans\text{-}[Cr(CO)_4(P(OPh)_3)_2] \rightleftarrows cis\text{-}[Cr(CO)_4(P(OPh)_3)_2] \quad (20)$$

(e) *fac*-$[Cr(CO)_3(P(OMe)_3)_3]$. On the short time scale of cyclic voltammetry the overall redox process at 22 °C for *fac*-$[Cr(CO)_3(P(OMe)_3)_3]$ is[15]

$$\begin{array}{ccc} fac\text{-}[Cr(CO)_3(P(OMe)_3)_3] & \rightleftharpoons & fac\text{-}[Cr(CO)_3(P(OMe)_3)_3]^+ + e^- \\ \uparrow \text{slow} & & \downarrow \text{fast} \\ mer\text{-}[Cr(CO)_3(P(OMe)_3)_3] & \rightleftharpoons & mer\text{-}[Cr(CO)_3(P(OMe)_3)_3]^+ + e^- \end{array} \quad (21)$$

However, in previous work a possible catalytic scheme for the reaction *fac* ⇄ *mer* was noted,[15] and this has now been investigated in detail. Controlled-potential oxidative electrolysis of a freshly prepared solution of colorless *fac*-$[Cr(CO)_3(P(OMe)_3)_3]$ at 0.6 V vs. Ag/AgCl produces a yellow solution whose reductive cyclic voltammogram is identical with that shown in Figure 2b for the *mer*-$[Cr(CO)_3(P(OMe)_3)_3]^{+/0}$ redox couple. As expected, the reductive controlled-potential electrolysis of the oxidized solution produces a colorless solution and an oxidative cyclic voltammogram identical with that shown in Figure 3 with two oxidation responses in the range 0–0.6 V vs. Ag/AgCl. Infrared monitoring of the oxidative electrolysis experiment indicates rapid conversion of *fac*-$[Cr(CO)_3(P(OMe)_3)_3]$ to the *mer* isomer at an early stage of the electrolysis, which must be occurring via a catalytic process.

The $NOPF_6$ oxidation of freshly prepared solutions of *fac*-$[Cr(CO)_3(P(OMe)_3)_3]$ was monitored at 22 °C by using a platinum rotating disk electrode (Figure 4) and infrared spectroscopy (not shown). Figure 4a shows the oxidative scan prior to the addition of $NOPF_6$. The $E_{1/2}$ value of this oxidation corresponds to that calculated from the oxidative cyclic voltammogram of pure *fac*-$[Cr(CO)_3(P(OMe)_3)_3]$. The first scan, recorded within 1 min of the addition of a small amount of $NOPF_6$ (Figure 4b), showed that the current caused by the oxidation of *fac*-$[Cr(CO)_3(P(OMe)_3)_3]$ had lessened, while another oxidation was observed with an $E_{1/2}$ value corresponding to the oxidation of *mer*-$[Cr(CO)_3(P(OMe)_3)_3]$. This is a surprising result since the rate of isomerization of *fac*-$[Cr(CO)_3P(OMe)_3)_3]$ to *mer*-$[Cr(CO)_3(P(OMe)_3])_3]$ is relatively slow (as demonstrated by letting the pure compound stand in dichloromethane solution), and this suggests that a catalytic process involving small amounts of *mer*-$[Cr(CO)_3(P(OMe)_3)_3]^+$ must be operative. The chemical oxidation was monitored until 100% *mer*-$[Cr(CO)_3(P(OMe)_3)_3]^+$ was produced (Figure 4d). The solution at the conclusion of the oxidation was yellow. These results indicate that upon chemical, as well as electrochemical, oxidation the product finally observed

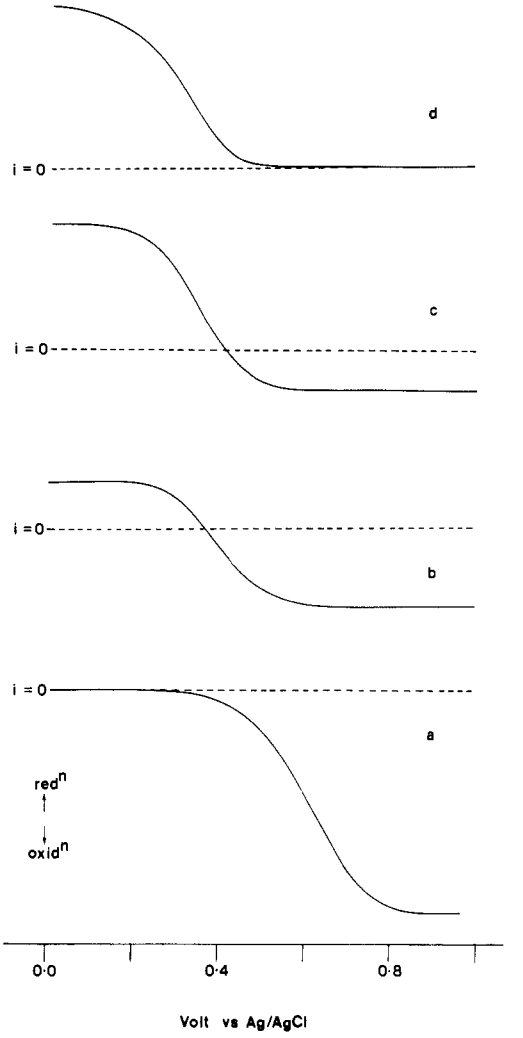

Figure 4. Voltammograms at a platinum rotating disk electrode (2000 cycles/min) monitoring the course of oxidation of ≃2 × 10^{-4} M *fac*-$[Cr(CO)_4(P(OMe)_3)_3]$ by $NOPF_6$ at 22 °C in dichloromethane (a) prior to addition of $NOPF_6$, (b and c) during intermediate stages of reaction, and (d) at completion of the reaction.

is *mer*-$[Cr(CO)_3(P(OMe)_3)_3]^+$.

The oxidation of *fac*-$[Cr(CO)_3(P(OMe)_3)_3]$ with *trans*-$[Cr(CO)_4(P(OPh)_3)_2]^+$ produced analogous data. *trans*-$[Cr(CO)_4(P(OPh)_3)_2]^+$ was generated by oxidative controlled-potential electrolysis at 1.3 V vs. Ag/AgCl. The addition of aliquots of 10^{-4} M solutions of *trans*-$[Cr(CO)_4(P(OPh)_3)_2]^+$ to *fac*-$[Cr(CO)_3(P(OMe)_3)_3]$ in CH_2Cl_2 was monitored with a platinum rotating disk electrode. Figure 5a shows the oxidative scan of *fac*-$[Cr(CO)_3(P(OMe)_3)_3]$ before the addition of any *trans*-$[Cr(CO)_4(P(OPh)_3)_2]^+$. The second scan (Figure 5b), 40 s after addition of less than a stoichiometric amount of *trans*-$[Cr(CO)_4(P(OPh)_3)_2]^+$, reveals that two oxidation processes in the range 0–0.6 V vs. Ag/AgCl are now occurring at the platinum electrode. The $E_{1/2}$ values correspond to those for the oxidations of *fac*- and *mer*-$[Cr(CO)_3(P(OMe)_3)_3]$. *mer*-$[Cr(CO)_3(P(OMe)_3)_3]$ has been rapidly generated via the catalytic process. It is evident that any oxidant capable of generating *mer*-$[Cr(CO)_3(P(OMe)_3)_3]^+$ is appropriate for initiating the catalysis. After equimolar proportions of *fac*-$[Cr(CO)_3(P(OMe)_3)_3]$ and *trans*-$[Cr(CO)_4(P(OPh)_3)_2]^+$ were mixed, there remains no evidence of the *fac*-$[Cr(CO)_3(P(OMe)_3)_3]$ oxidation and only evidence for the respective $mer^{+/0}$ or $trans^{+/0}$ couples. That is, a quantitative reaction

$$trans\text{-}[Cr(CO)_4(P(OPh)_3)_2]^+ + fac\text{-}[Cr(CO)_3(P(OMe)_3)_3] \rightarrow trans\text{-}[Cr(CO)_4(P(OPh)_3)_2] + mer\text{-}[Cr(CO)_3(P(OMe)_3)_3]^+ \quad (22)$$

has occurred. As expected, the addition of further *trans*-[Cr-

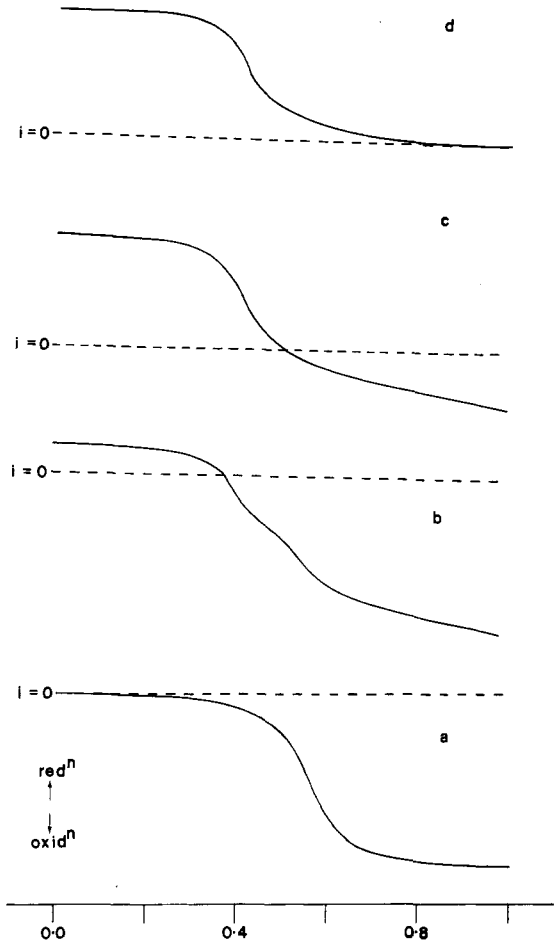

Figure 5. Voltammograms at a platinum rotating disk electrode (2000 cycles/min) monitoring the reaction of $\simeq 10^{-4}$ M *fac*-$[Cr(CO)_3(P(OMe)_3)_3]$ with *trans*-$[Cr(CO)_4(P(OPh)_3)_2]^+$ in dichloromethane at 22 °C (a) prior to addition of *trans*-$[Cr(CO)_4(P(OPh)_3)_2]^+$, (b) after addition of a less than stoichiometric amount of *trans*-$[Cr(CO)_4(P(OPh)_3)_2]^+$, (c) after addition of close to a stoichiometric amount of *trans*-$[Cr(CO)_4(P(OPh)_3)_2]^+$, and (d) after addition of a stoichiometric amount of *trans*-$[Cr(CO)_4(P(OPh)_3)_2]^+$.

$(CO)_4(P(OPh)_3)_2]^+$ at the completion of the reaction has no effect on the shape of the oxidation scan under conditions of cyclic voltammetry.

Oxidative cyclic voltammograms of a solution of *fac*-$[Cr(CO)_3(P(OMe)_3)_3]$ were also obtained as a function of time at 22 °C (Figure 6). The initial cyclic voltammograms at $t = 0$ of the freshly prepared solution shows the pure *fac* oxidation wave and the *mer* reduction wave on reverse scans as seen previously. Further voltammograms were obtained at intervals over a total time period of 2.5 h. During this time it was observed that an oxidation peak corresponding to that of the oxidation of *mer*-$[Cr(CO)_3(P(OMe)_3)_3]$ appeared and increased in intensity while the peak for the oxidation of *fac*-$[Cr(CO)_3(P(OMe)_3)_3]$ diminished in size, indicating that upon standing the 18-electron *fac*-$[Cr(CO)_3(P(OMe)_3)_3]$ slowly isomerizes to the corresponding 18-electron *mer*-$[Cr(CO)_3(P(OMe)_3)_3]$ complex. An equilibrium appeared to have been reached in approximately 2 h. These data serve to emphasize the catalytic nature of the processes forming *mer*-$[Cr(CO)_3(P(OMe)_3)_3]$ on controlled-potential electrolysis or addition of $NOPF_6$ or *trans*-$[Cr(CO)_4(P(OPh)_3)_2]^+$ to *fac*-$[Cr(CO)_3(P(OMe)_3)_3]$ as described above. To ensure that there was no significant effect on this isomerization process from the very small amounts of 17-electron cation remaining after cyclic voltammetric experiments, a control solution was prepared and kept under nitrogen and in darkness. The cyclic voltammogram of this solution after 2.5 h was identical with that of the monitored solution.

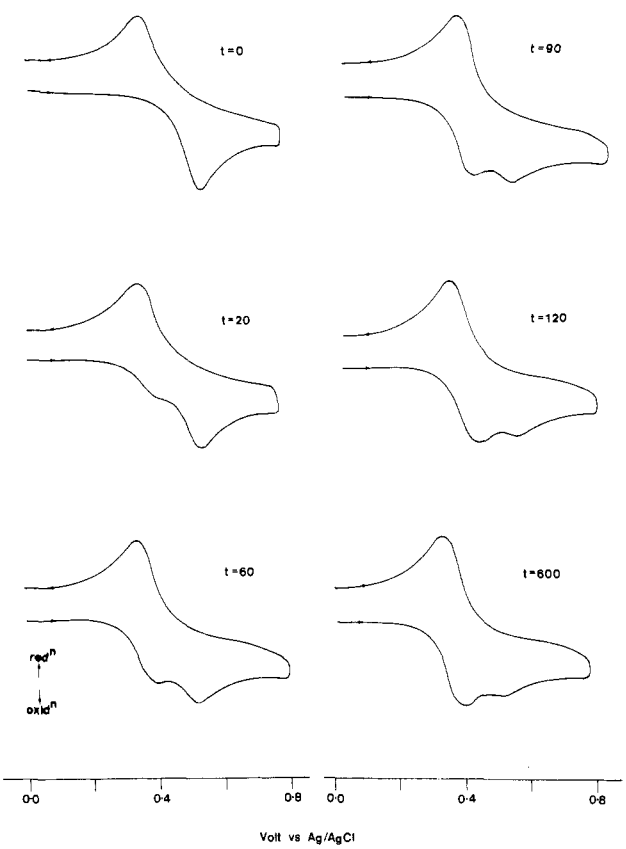

Figure 6. Cyclic voltammograms (scan rate = 200 mV/s) for the oxidation of initially 2×10^{-4} M *fac*-$[Cr(CO)_3(P(OMe)_3)_3]$ as a function of time (in min) in dichloromethane at 22 °C at a stationary platinum electrode.

(f) Thermodynamics and Kinetics of the *fac*/*mer*-$[Cr(CO)_3(P(OMe)_3)_3]^{+/0}$ Redox Couples. It was possible to determine all thermodynamic and kinetic parameters of the overall redox system described by

$$\begin{array}{ccc} fac\text{-}[Cr(CO)_3(P(OMe)_3)_3] & \rightleftharpoons & fac\text{-}[Cr(CO)_3(P(OMe)_3)_3]^+ \\ \Updownarrow & & \downarrow \\ mer\text{-}[Cr(CO)_3(P(OMe)_3)_3] & \rightleftharpoons & mer\text{-}[Cr(CO)_3(P(OMe)_3)_3]^+ \end{array} \quad (23)$$

From the series of cyclic voltammograms in the early stages of the reaction

$$fac\text{-}[Cr(CO)_3(P(OMe)_3)_2] \xrightarrow{k_1} mer\text{-}[Cr(CO)_3(P(OMe)_3)_3] \quad (24)$$

concentration–time data consistent with first-order kinetics was obtained. The value of k_1 at 22 °C was calculated to be $(1.8 \pm 0.3) \times 10^{-4}$ s^{-1}. As noted earlier, catalysis is readily achieved, and the complete absence of oxidants and light is required to reproduce this data. At equilibrium, the concentrations of fac^0 and mer^0 are both readily calculated from the observed electrochemical response. The value of K_1 at 22 °C for

$$fac\text{-}[Cr(CO)_3(P(OMe)_3)_3] \overset{K_1}{\rightleftharpoons} mer\text{-}[Cr(CO)_3(P(OMe)_3)_3] \quad (25)$$

is 4.0 ± 0.5; i.e., the mer^0 isomer is favored. From the relationship

$$K_1 = k_1/k_{-1} \quad (26)$$

the value of k_{-1} was calculated to have a value of $(4.5 \pm 1.3) \times 10^{-5}$ s^{-1}.

Assuming that the reversible $E^r_{1/2} = E^0$ for the *fac*-$[Cr(CO)_3(P(OMe)_3)_3]^{+/0}$ and *mer*-$[Cr(CO)_3(P(OMe)_3)_3]^{+/0}$ couples, the equilibrium constant, K_3, for the redox cross-reaction

$$fac\text{-}[Cr(CO)_3(P(OMe)_3)_3]^+ + mer\text{-}[Cr(CO)_3(P(OMe)_3)_3] \overset{K_3}{\rightleftharpoons} fac\text{-}[Cr(CO)_3(P(OMe)_3)_3] + mer\text{-}[Cr(CO)_3(P(OMe)_3)_3]^+ \quad (27)$$

was calculated to have a value of 160 ± 13 at 22 °C. This value indicates that in the redox sense the species *fac*-$[Cr(CO)_3(P(OMe)_3)_3]$ and *mer*-$[Cr(CO)_3(P(OMe)_3)_3]^+$ are favored. Since

$$K_3 = \frac{[fac][mer^+]}{[mer][fac^+]} = K_2/K_1 \quad (28)$$

and the value of K_1 is known (see above), the value of K_2 for the reaction

$$fac\text{-}[Cr(CO)_3(P(OMe)_3)_3]^+ \overset{K_2}{\rightleftharpoons} mer\text{-}[Cr(CO)_3(P(OMe)_3)_3]^+ \quad (29)$$

could be calculated and has a value of 640 ± 130. This value clearly shows that thermodynamically the 17-electron *mer*-$[Cr(CO)_3(P(OMe)_3)_3]^+$ species is favored with respect to the fac^+ isomer far more than the corresponding 18-electron mer^0 is favored over fac^0, in accordance with the predictions of Mingos.[4]

The series of cyclic voltammograms for the oxidation of *fac*-$[Cr(CO)_3(P(OMe)_3)_3]$ obtained at varying temperatures over the range 0 to −60 °C enables the activation parameters and the value of k_2 to be determined by using equations described by Nicholson and Shain.[19] The activation energy (E_A = 15.9 ± 0.7 kJ/mol) and entropy of activation (ΔS^* = −17.0 ± 1.0 J/(K mol)) are consistent with an intramolecular twist mechanism.[20] The use of an Arrhenius plot and the relationship

$$K_2 = k_2/k_{-2} \quad (30)$$

where k_2 and k_{-2} are defined by

$$fac\text{-}[Cr(CO)_3(P(OMe)_3)_3]^+ \underset{k_{-2}}{\overset{k_2}{\rightleftharpoons}} mer\text{-}[Cr(CO)_3(P(OMe)_3)_3]^+ \quad (31)$$

enables kinetic data to be obtained at 22 °C for these reactions. The values of k_2 and k_{-2} are 0.11 ± 0.01 and (1.7 ± 0.8) × 10^{-4} s^{-1}, respectively. The value of k_{-2} is very much smaller than k_2, unlike the values of k_1 and k_{-1} described earlier, which are comparable in magnitude. However, despite the fact that k_{-2} is slow relative to k_2 it is still considerably faster than k_{-1}, showing that the isomerization in either direction for the 17-electron configuration is faster than for the 18-electron case in either direction. This suggests that enhanced isomerization rates are generally to be expected for the 17-electron configuration.

The observation of catalytic isomerization initiated either by $NOPF_6$, *trans*-$[Cr(CO)_4(P(OPh)_3)_2]^+$, or any other *trans*-$[Cr(CO)_4P_2]^+$ complex can be explained by a redox-based route (shown in eq 33–35) which occurs in competition with the slow intramolecular twist mechanism of the 18-electron species

$$fac\text{-}[Cr(CO)_3(P(OMe)_3)_3] \xrightarrow{\text{slow}} mer\text{-}[Cr(CO)_3(P(OMe)_3)_3] \quad (32)$$

The proposed alternative route involving a 17-electron cation is

$$fac\text{-}[Cr(CO)_3(P(OMe)_3)_3] \xrightarrow{\text{oxidant}} fac\text{-}[Cr(CO)_3(P(OMe)_3)_3]^+ \quad (33)$$

$$fac\text{-}[Cr(CO)_3(P(OMe)_3)_3]^+ \xrightarrow{k_2} mer\text{-}[Cr(CO)_3(P(OMe)_3)_3]^+ \quad (34)$$

$$\begin{array}{ccc} mer\text{-}[Cr(CO)_3L_3]^+ & + & fac\text{-}[Cr(CO)_3L_3]^0 \\ \uparrow k_2 & & \downarrow k_1 \\ fac\text{-}[Cr(CO)_3L_3]^+ & + & mer\text{-}[Cr(CO)_3L_3]^0 \end{array} \quad (35)$$

where L = $P(OMe)_3$, and at 22 °C k_1 = (1.8 ± 0.3) × 10^{-4} s^{-1} and k_2 = 0.11 ± 0.01 s^{-1}.

Thus, *mer*-$[Cr(CO)_3(P(OMe)_3)_3]^+$ is generated via oxidation of *fac*-$[Cr(CO)_3(P(OMe)_3)_3]$ to *fac*-$[Cr(CO)_3(P(OMe)_3)_3]^+$ (eq 33) followed by isomerization (eq 34). This initiates the redox cross-reaction (eq 35), even though (35) in the direction written is thermodynamically unfavored. This provides an alternative and faster pathway for the isomerization of *fac*-$[Cr(CO)_3(P(OMe)_3)_3]$ to *mer*-$[Cr(CO)_3(P(OMe)_3)_3]$. This catalytic reaction occurs in parallel with the direct isomerization described by eq 32.

(g) fac/mer-$[Cr(CO)_3(P(OEt)_3)_3]^{+/0}$. The behavior of the *fac*- and *mer*-$[Cr(CO)_3(P(OEt)_3)_3]$ complexes is very similar to that described above for the *fac*- and *mer*-$[Cr(CO)_3(P(OMe)_3)_3]$ complexes. Some of the spectral and electrochemical data are summarized in Tables I and II. Quantitative aspects of the thermodynamics and kinetics of this system were not examined, but are qualitatively similar to those of the trimethyl phosphite analogue.

Registry No. *trans*-$[Cr(CO)_4(PPh_3)_2]$, 38800-75-8; *trans*-$[Cr(CO)_4(P(m\text{-}tol)_3)_2]$, 36491-14-2; *trans*-$[Cr(CO)_4(P(p\text{-}tol)_3)_2]$, 36537-70-9; *trans*-$[Cr(CO)_4(P(OPh)_3)_2]$, 35039-06-6; *trans*-$[Cr(CO)_4(P(OEt)_3)_2]$, 19998-74-4; *trans*-$[Cr(CO)_4(P(OMe)_3)_2]$, 21370-42-3; *mer*-$[Cr(CO)_3(P(OMe)_3)_3]$, 30571-27-8; *cis*-$[Cr(CO)_4(P(OEt)_3)_2]$, 19998-73-3; *cis*-$[Cr(CO)_4(P(OMe)_3)_2]$, 16027-43-3; *cis*-$[Cr(CO)_4(P(OPh)_3)_2]$, 77551-77-0; *fac*-$[Cr(CO)_3(P(OMe)_3)_3]$, 17764-72-6; *trans*-$[Cr(CO)_4(PPh_3)_2]^+$, 86475-63-0; *trans*-$[Cr(CO)_4(P(p\text{-}tol)_3)_2]^+$, 100165-41-1; *trans*-$[Cr(CO)_4(P(OPh)_3)_2]^+$, 100165-42-2; *trans*-$[Cr(CO)_4(P(OEt)_3)_2]^+$, 100165-43-3; *trans*-$[Cr(CO)_4(P(OMe)_3)_2]^+$, 100165-44-4; *mer*-$[Cr(CO)_3(P(OMe)_3)_3]^+$, 90064-72-5; *mer*-$[Cr(CO)_3(P(OEt)_3)_3]$, 100227-62-1; *fac*-$[Cr(CO)_3(P(OEt)_3)_3]$, 24564-35-0; *trans*-$[Cr(CO)_4(P(m\text{-}tol)_3)_2]^+$, 100165-45-5; *mer*-$[Cr(CO)_3(P(OEt)_3)_3]^+$, 100165-46-6; *fac*-$[Cr(CO)_3(P(OEt)_3)_3]^+$, 100227-63-2; *fac*-$[Cr(CO)_3(P(OMe)_3)_3]^+$, 100227-64-3.